

# Pharmacokinetics and Biodistribution of Thymoquinone-loaded Nanostructured Lipid Carrier After Oral and Intravenous Administration into Rats

This article was published in the following Dove Press journal:  
International Journal of Nanomedicine

Fatin Hannani Zakarial Ansar<sup>1</sup>  
Saiful Yazan Latifah<sup>1,2</sup>  
Wan Hamirul Bahrin Wan  
Kamal<sup>3</sup>  
Khei Choong Khong<sup>3</sup>  
Yen Ng<sup>3</sup>  
Jia Ning Foong<sup>1</sup>  
Banulata Gopalsamy<sup>2</sup>  
Wei Keat Ng<sup>1</sup>  
Chee Wun How<sup>4</sup>  
Yong Sze Ong<sup>1</sup>  
Rasedee Abdullah<sup>2,5</sup>  
Mohd Yusmaidie Aziz<sup>6</sup>

<sup>1</sup>Laboratory of Molecular Medicine, Institute of Bioscience, Universiti Putra Malaysia, Serdang, Selangor, Malaysia; <sup>2</sup>Department of Biomedical Science, Faculty of Medicine and Health Sciences, Universiti Putra Malaysia, Serdang, Selangor, Malaysia; <sup>3</sup>Laboratory of Preclinical Study, Block 24, Medical Technology Division, Malaysian Nuclear Agency, Kajang, Selangor, Malaysia; <sup>4</sup>Laboratory of Vaccines and Immunotherapeutics, Institute of Bioscience, Universiti Putra Malaysia, Serdang, Selangor, Malaysia; <sup>5</sup>Department of Veterinary Pathology and Microbiology, Faculty of Veterinary Medicine, Universiti Putra Malaysia, Serdang, Selangor, Malaysia; <sup>6</sup>Advanced Medical and Dental Institute, University of Science Malaysia, Kepala Batas, Pulau Pinang, Malaysia

Correspondence: Saiful Yazan Latifah;  
Wan Hamirul Bahrin Wan Kamal  
Tel +60 3 89472308  
Fax +60 3 89436178  
Email latifahsy@upm.edu.my;  
mirul@nuclearmalaysia.gov.my

**Background:** Thymoquinone (TQ), an active compound isolated from *Nigella sativa*, has been proven to exhibit various biological properties such as antioxidant. Although oral delivery of TQ is valuable, it is limited by poor oral bioavailability and low solubility. Recently, TQ-loaded nanostructured lipid carrier (TQ-NLC) was formulated with the aim of overcoming the limitations. TQ-NLC was successfully synthesized by the high-pressure homogenization method with remarkable physiochemical properties whereby the particle size is less than 100 nm, improved encapsulation efficiency and is stable up to 24 months of storage. Nevertheless, the pharmacokinetics and biodistribution of TQ-NLC have not been studied. This study determined the bioavailability of oral and intravenous administration of thymoquinone-loaded nanostructured lipid carrier (TQ-NLC) in rats and its distribution to organs.

**Materials and Methods:** TQ-NLC was radiolabeled with technetium-99m before the administration to the rats. The biodistribution and pharmacokinetics parameters were then evaluated at various time points. The rats were imaged at time intervals and the percentage of the injected dose/gram (%ID/g) in blood and each organ was analyzed.

**Results:** Oral administration of TQ-NLC exhibited greater relative bioavailability compared to intravenous administration. It is postulated that the movement of TQ-NLC through the intestinal lymphatic system bypasses the first metabolism and therefore enhances the relative bioavailability. However, oral administration has a slower absorption rate compared to intravenous administration where the AUC<sub>0-∞</sub> was 4.539 times lower than the latter.

**Conclusion:** TQ-NLC had better absorption when administered intravenously compared to oral administration. However, oral administration showed greater bioavailability compared to the intravenous route. This study provides the pharmacokinetics and biodistribution profile of TQ-NLC in vivo which is useful to assist researchers in clinical use.

**Keywords:** thymoquinone, nanostructured lipid carrier, bioavailability, biodistribution, pharmacokinetics

## Introduction

The emergence of nanotechnology has principally benefitted the medical field, specifically for diagnostic and therapeutic purposes.<sup>1-5</sup> Currently, nanoparticle-based drugs such as polymers and lipids have flooded the pharmaceutical research world in search for the best candidate for treatment and management of numerous ailments.<sup>3,6-9</sup> The first generation of novel colloidal drug carriers developed to enhance parenteral delivery were polymeric nanoparticles.<sup>5-10</sup> However the use of

polymeric nanoparticles could possibly encounter toxicity, were deemed uneconomical and difficult when rescaled.<sup>8</sup> Lipid-based nanoparticles have magnetized attention in the industrial and academic fields as a potential substitution to polymeric nanoparticles due to its more natural composition that is extremely biodegradable and biocompatible in vivo.<sup>11</sup>

*Nigella sativa* is a medicinal plant also known as black seed or *Habbatus sauda*.<sup>12</sup> It is a grassy annual herb that belongs to the Ranunculaceae family. It is a native plant in India, Pakistan, Middle and Far Eastern countries.<sup>13,14</sup> *N. sativa* seeds are commonly used by old folk in the community as nutritional supplements in the form of spices and food preservatives.<sup>13,15</sup> Thymoquinone (TQ) is the bioactive compound containing the majority of the biological activities of *N. sativa* seed<sup>16</sup> such as antioxidant, anti-inflammatory<sup>17</sup> and neuroprotective.<sup>18</sup>

Animal studies employing TQ via the intraperitoneal route reported desired effect of the drug. But when this research is translated for preclinical and clinical use, this mode of administration might not be ideal due to the discomfort felt by patients, not cost effective and concerns on the aseptic techniques used.<sup>19</sup> A noninvasive oral route is therefore preferred for drug delivery. However, the delivery of TQ via oral administration is largely restricted by the solubility-related poor oral bioavailability<sup>19</sup> and the relatively low solubility of pure TQ in water.<sup>20</sup>

As TQ is a hydrophobic molecule, numerous studies have attempted to encapsulate TQ into nanoformulation. Lipid-based nanoparticles are highly biodegradable and bioacceptable making them less toxic compared to others. TQ has been successfully encapsulated into NLC.<sup>21</sup> The NLC is characterized as an enhanced formulation of lipid generation developed from solid lipid nanoparticle (SLN) with better and upgraded characteristics.<sup>22</sup> These lipid-based nanoparticles are mainly synthesized using a high-pressure homogenizer and can produce particle dispersions with up to 80% solid composition.<sup>23–25</sup> NLC comprises of a mixture of lipid in the solid and liquid form which enhances the structure of lipid based nanoparticles.<sup>23</sup> Throughout the process of synthesizing NLC, highly disordered and defective lipid matrices were formed by the distinctively structured lipids. This provides enormous molecular cavities for drug molecules<sup>23,26</sup> thus ensuring higher drug loading capacity and preserved drug stability during storage.<sup>27–29</sup>

One vital fact about the in vivo use of nanoparticles, in particular TQ-NLC, is the study of its pharmacokinetics and

biodistribution. The physiochemical characteristics of TQ-NLC in vitro and in vivo is well studied, but to date there are no reports on the in vivo pharmacokinetics, biodistribution, organ accumulation, and elimination.<sup>5,930–32</sup>

Different nuclear medicine techniques are exploited for pharmacokinetics and biodistribution studies of nanoparticles. These techniques are based on emissions which source from the electromagnetics emission from radioisotopes distributed in vivo.<sup>33</sup> Radioisotopes mainly used in nuclear medicine include iodine-131, indium-111, thallium-201, fluorine-18, technetium-99m, gallium-67 and others.<sup>34–36</sup> One of the most frequently used radiotracers for imaging is technetium-99m ( $Tc^{99m}$ ), which is abundantly used in nuclear medicine laboratories. It is also cost effective and has suitable physical and chemical properties including a physical half-life of 6.02 hours and low energy of gamma emission (140 keV).<sup>36–40</sup> Using  $Tc^{99m}$  to tag TQ-NLC, this study evaluated the pharmacokinetics and tissue distribution of TQ-NLC in rats following oral and intravenous administration. This outcome provides vital information to establish TQ-NLC as a drug and for future biomedical applications.

## Materials and Methods

### Materials

$NaTcO_4$  ( $^{99m}TcO_4^-$ ) was attained from a  $^{99}Mo/Tc^{99m}$  generator (Drytec™) purchased from GE Healthcare Bio-Sciences, UK. Stannous chloride was obtained from Sigma Chemicals, St Louis, MO, USA. Ultrapure water was obtained from a Milli-Q\_Plus apparatus (Millipore). All other chemicals used in the experiment were analytical grade.

### Preparation of TQ-NLC

TQ-NLC was synthesised as outlined previously by Ng et al<sup>21</sup> by using a high-pressure homogenization technique. There were two phases involved in the production of TQ-NLC that include lipid and aqueous phases. The lipid phase was prepared by mixing hydrogenated palm oil (Wilfarin™ hydrogenated refined palm oil; Wilmar International Limited, Neil Road, Singapore), lecithin (Phospholipon® 90G; Lipoid GmbH, Ludwigshafen, Germany) and olive oil. The mixture was heated up to 70°C and stirred with a Teflon-coated magnet until melted. The aqueous phase was prepared by dissolving sorbitol, Polysorbate 80 (Tween® 80; Sigma-Aldrich, St Louis, MO, USA) and thimerosal in deionized water. The mixture

was then heated to 70°C and added to the lipid phase with constant stirring. Prior to mixing both matrices, TQ was added and dissolved into the hot lipid phase solution. Further diminution was accelerated by a high-shear Ultra-Turrax dispersion mixer Ultra-Turrax® (IKA-werke, GmBH, Germany) at 13,000 rpm for 10 min with constant stirring at 70°C. The resulting hot pre-emulsion was further processed and homogenized by a high-pressure homogenizer EmulsiFlex (Avestin, Inc., Ottawa, Canada) at 1000 bars for 20 cycles. Finally, the nanoformulation (TQ-NLC) was allowed to cool down to room temperature for recrystallization.

## Characterisation of TQ-NLC

TQ-NLC was characterized based on the mean diameter, polydispersity index (PDI), and zeta potential. All the parameters were determined by using Zetasizer Nano ZS (Malvern Instruments GmbH, Herrenberg, Germany). Briefly, TQ-NLC was diluted with deionized water at a ratio of 1:9 and the parameters were read three times.

## Determination of TQ-NLC Encapsulation Efficiency (EE) and Drug Loading (DL) Capacity

Encapsulation efficiency (EE) and drug loading (DL) capacity were evaluated by ultrafiltration technique. Briefly, the separation of free TQ from TQ-NLC was done by using an ultrafilter (Amicon® Ultra, molecular weight cutoff [MWCO]: 10 kDa; EMD Millipore, Billerica, MA, USA) and centrifuged for 10 min at 2000 × g. High-performance liquid chromatography (HPLC) analysis was used to measure the amount of free TQ from TQ-NLC. Both EE and DL capacity were measured using the following formula:

$$EE(\%) = \frac{\text{Total amount of TQ in TQ-NLC} - \text{Free amount of TQ}}{\text{Total amount of TQ in TQ-NLC}} \times 100$$

$$DL(\%) = \frac{\text{Amount of TQ entrapped in TQ-NLC}}{\text{Amount of entrapped in TQ-NLC} + \text{Excipients}} \times 100$$

HPLC analysis was carried out using a Waters Alliance HPLC System (Milford, MA, USA) equipped with a photodiode array detector. The stationary phase consists of a Merck HSS-T-3 C18 (100×2.1 mm, 1.8 mm) and the HPLC column was maintained at 30°C. A mixture of

methanol (70%) and water (30%) acts as mobile phase which was pumped at a flow rate of 1.0 mL/min. The HPLC analysis was conducted at 255 nm wavelength with a total run time of five minutes and the volume of injection was 10 µL. Data acquisition, data handling, and instrument control were performed by Empower Software v1.0. (Milford).

## In vitro Release Modelling of TQ-NLC

The in vitro drug release profile analysis of pure TQ solution (solubilized in ethanol) and TQ-NLC was performed over 72 h using the dialysis bag diffusion technique.<sup>31</sup> Prior to the test, a dialysis bag with MWCO of 14 kDa (Sigma-Aldrich, USA) was kept overnight in the dissolution medium (2.0% SDS in PBS) to ensure thorough wetting of the membrane. Pure TQ solution or TQ-NLC (2 mL of each) was added into its respective dialysis bag and then transferred into a beaker containing 45 mL of dissolution medium. The beaker was placed at 37°C on an incubator shaker (100 rpm) (Sartorius, Germany). At 0, 0.0167, 0.0333, 0.0833, 0.1667, 0.3333, 0.5, 1, 2, 4, 8, 12, 18, 24, 48 and 72 h, 1 mL of the medium was withdrawn. The same amount of fresh dissolution medium was added as a replacement to ensure constant volume was maintained. The samples were diluted in HPLC grade methanol (1:1) and analysed by HPLC (Waters, USA). Mathematical modelling was performed by using the parameters that provided the closest fit between experimental observation and the nonlinear function to various releases (zero order, first order, Higuchi, and Hixson–Crowell) to understand the mechanism of drug release from TQ-NLC.<sup>41,42</sup>

## Radiolabelling Formulations

Direct labeling method was implied to radiolabel TQ-NLC with Tc<sup>99m</sup> by using stannous chloride (SnCl<sub>2</sub> H<sub>2</sub>O) as a reducing agent under nitrogen atmosphere.<sup>34</sup> In order to prevent the hydrolysis of Sn<sup>2+</sup> and formation of radiocolloids (reduced and hydrolyzed Tc<sup>99m</sup>), ascorbic acid was integrated in the direct labeling method as an antioxidant that comprised weak acid pH. In brief, aqueous solution containing SnCl<sub>2</sub> H<sub>2</sub>O (1%) and ascorbic acid (5%) were added to the TQ-NLC suspension and mixed under nitrogen atmosphere. Approximately 1 to 1.5 mCi of Tc<sup>99m</sup>-eluate (1 mCi) was obtained from a commercial <sup>99</sup>Mo/Tc<sup>99m</sup> generator (Drytec™) and added into the vial with constant nitrogen atmosphere. The reaction mixture was moderately stirred and incubated at room temperature for 10 min. Next, 0.5 M sodium bicarbonate (NaHCO<sub>3</sub>) was added to the radiolabelled TQ-NLC suspension in order to attain a pH of

five. The amount of  $\text{SnCl}_2 \cdot \text{H}_2\text{O}$  was optimized to obtain maximum percentage of radiolabeled of TQ-NLC suspension.

### Optimization of Radiolabeling Efficiency

The amount of  $\text{SnCl}_2 \cdot \text{H}_2\text{O}$  of the radiolabeled suspension was optimized by changing one parameter at a time and by performing quality control tests for the radiolabeled suspension.<sup>43</sup> A range of 50–600  $\mu\text{g/mL}$  of stannous chloride was added to optimize the amount of  $\text{SnCl}_2 \cdot \text{H}_2\text{O}$  that affects the percentage of labeling efficiency of the suspension.

### Determination of Labeling Efficiency

The labeling efficiency and stability of the radiolabeled suspension was determined using an instant thin layer chromatography (iTLC). After final preparation of radiolabeled TQ-NLC, the radiolabeling stability was recorded up to 24 h.<sup>43</sup> The iTLC was performed using instant thin layer chromatography silica gel impregnated glass fiber sheets to determine free technetium and percentage of radiocolloids in the preparation. An amount of 3  $\mu\text{L}$  of the radiolabeled suspension was spotted at 1 cm from the bottom (origin). To determine the amount of free  $\text{Tc}^{99\text{m}}$  pertechnetate and reduced/hydrolyzed (R/H)  $\text{Tc}^{99\text{m}}$ , these strips were developed using acetone as mobile phase and a solvent system. The solvent front was permitted to reach a height of approximately 8 cm from the origin and the strip was measured using a TLC scanner (AR 2000, Bioscan, USA). The free pertechnetate existing in the suspension migrated to the top portion of the strips while the radiocolloids (reduced/hydrolyzed technetium) with radiolabeled suspension stayed at the origin of the strips where the suspension was applied. A mixture of pyridine:acetic acid:water at a ratio of 3:5:1.5 was used to determine the existence of radiocolloids in the radiolabeled suspension. The radiocolloids remain at the origin while both free pertechnetate and radiolabeled complex migrated together with the solvent front. Hence, the radiolabeling efficiency was calculated by subtracting the total of free pertechnetate and reduced/hydrolyzed technetium by 100%.<sup>44,45</sup>

### Stability of Labeled Complex

Stability of the TQ-NLC labelled  $\text{Tc}^{99\text{m}}$  complex was determined in vitro in rat serum by ascending TLC technique. Briefly, 0.1 mL of the labeled complex was incubated with 0.9 mL freshly collected rat serum at 37°C.

Incubated mixture of the labeled suspension and rat serum was spotted at iTLC strips at time intervals of 1, 2, 4, 6, 8, 24 h. The spotted strips were counted using an automated TLC scanner and the percentage of labelling efficiency of radiolabeled TQ-NLC was measured for free  $\text{Tc}^{99\text{m}}$  and reduced/hydrolyzed technetium as well as radiocolloids.

### Experimental Animals

Healthy male Sprague Dawley rats (180–200 gm) were used for pharmacokinetics and biodistribution studies. Prior to experimentation, the animals were randomly divided into two groups for different routes of administration (oral and intravenous injection). They were housed in cages under standard laboratory conditions, with a period of 12-hr light/12-h darkness cycle, at 20°C–24°C with 40%–50% relative humidity. The animals were acclimatized for one week prior to the experiment. The rats were fed with standard chow pellet (Specialty Feeds, Glen Forrest, WA, Australia) and allowed to drink water ad libitum. Each group was further divided according to different time point (n=6). All the experimental procedures were reviewed and approved by the Institutional Animal Care and Use Committee (IACUC), Universiti Putra Malaysia (UPM/IACUC/AUP-R085/2017) and followed Canadian Council on Animal Care Guide to the Care and Use of Experimental Animals.

### Pharmacokinetics Study

The pharmacokinetics study was conducted in accordance with Organisation for Economic Co-operation and Development (OECD) 417 Guideline for Testing of Chemicals. The rats were administered with  $^{99\text{m}}\text{Tc}$ -TQ-NLC dispersion by oral gavage and intravenous injection at the dose of 100 mg/kg<sup>22,46</sup> and 25 mg/kg,<sup>47</sup> respectively, and later anesthetized by inhalation of 4.0% isoflurane (2500 cc/min). The gamma ray whole-body data was acquired at different time points (0.25, 0.5, 1, 2, 4, 6, 8, 12 and 24 h) after the oral administration and 0.25, 0.5, 1, 2, 4, 6 and 24 h following intravenous administration. Blood was collected into heparin (for plasma) and plain tube via cardiac puncture. Both the blood samples were placed in pre-weighed tubes and analyzed using shielded well-type gamma scintillation counter. Radioactivities in the samples were determined in the units of counts. A series of diluted free  $\text{Tc}^{99\text{m}}$  solution were prepared and counted using a gamma counter to obtain the radioactivity correction factor for further use in the animal biodistribution data analysis. Area under the curve (AUC), relative bioavailability,

elimination half-life, volume of distribution and other pharmacokinetic parameters were calculated by noncompartmental analysis model using WinNonlin v6.1 (Certara, MO, USA). Relative bioavailability of TQ-NLC was calculated by the following equation;

$$\text{Relative bioavailability} = \left\{ \frac{\text{AUC}_{0-\infty}}{\text{AUC}_{0-\infty \text{ suspension}}} \right\} \times 100$$

AUC<sub>0-∞</sub>: Area under the curve for TQ-NLC suspension

## Biodistribution Study

The biodistribution study was conducted in accordance with Organisation for Economic Co-operation and Development (OECD) 417 Guideline for Testing of Chemicals. The gamma ray whole-body data was acquired at 0.25, 0.5, 1, 2, 4, 6, 8, 12 and 24 h after the oral administration and 0.25, 0.5, 1, 2, 4, 6 and 24 h following the intravenous administration. The anesthetized rats were placed horizontally under a single-headed gamma camera (BHP 6602, Hamamatsu, China) employing a low energy gamma with high resolution collimator. Images were acquired at the end of the biodistribution studies. Different tissues/organs such as liver, kidney, heart, spleen, lungs, and brain were dissected, washed twice using normal saline, freed from adhering tissue/fluid and weighed. The radioactivity present in each tissue/organ was measured using a shielded well-type gamma scintillation counter (2470 Wizard, Perkin Elmer, USA). The %ID/g of each organ was calculated using the following equation in which ID represents the injected dose and M is the weight of each organ:

$$\% \text{ ID/organ weight} = \frac{\text{each count}}{\text{total count}} \times 100 / M$$

## Statistical Analysis

All statistical analyses were performed using GraphPad Prism version 6 (GraphPad Software, San Diego, CA,

USA). One-way ANOVA in multiple comparison followed by Tukey's post hoc test were applied to calculate the significant differences between groups. All data were obtained at least in triplicates and results are presented as mean ±SD unless stated otherwise. Value of  $P < 0.05$  was considered significant.

## Results

### Characteristics of TQ-NLC

The physiochemical characteristics of TQ-NLC are shown in Table 1. TQ-NLC has a uniform diameter of 37.84±0.287 nm at room temperature (25°C). The PDI for TQ-NLC was lower than 0.2 and the zeta potential was -5.80±0.450.

### TQ-NLC EE and DL Capacity

HPLC data of free TQ detected at a wavelength of 254 nm and 9.742 min retention time is shown in Table 2. From the HPLC analysis, 98.07% of TQ was encapsulated in the NLC and the DL was 8.72%.

### In vitro Release of TQ-NLC

Figure 1 shows that 46.95±0.40% of TQ was released from TQ-NLC after 72 h. The release of pure TQ solution was significantly higher ( $P < 0.05$ ) than TQ-NLC.

### Release Kinetic of Thymoquinone-loaded Nanostructured Lipid Carrier

Based on Table 3, the release of TQ from NLC best fitted to the zero-order model with the highest  $R^2$  value of 0.971, as compared to Higuchi (0.9328), Hixson-Crowell's (0.7627) and first order model (0.5708). The release exponent ( $n$ ) obtained from Korsmeyer-Peppas equation for TQ-NLC was 0.7136 (Figure 2).

**Table 1** Physiochemical Characteristics of TQ-NLC After 24 Hours

| Formulation | Z-Average (d, nm) | PDI        | Zeta Potential (mV) | Temperature (°C) |
|-------------|-------------------|------------|---------------------|------------------|
| TQ-NLC      | 37.84±0.287       | 0.19±0.003 | -5.80±0.450         | 25               |

**Note:** Values are expressed as mean ±SD and measured in triplicates.

**Abbreviations:** PDI, polydispersity index; TQ-NLC, thymoquinone-loaded nanostructured lipid carrier.

**Table 2** Free TQ Detected by HPLC at Wavelength of 254 Nm with Retention Time of 9.7 Minutes

| Peak Name | Retention Time (minutes) | Area       | % area | Height | Amount | Unit   |
|-----------|--------------------------|------------|--------|--------|--------|--------|
| Free TQ   | 9.742                    | 11,336,968 | 100    | 79,130 | 9.64   | mg/mL* |

**Note:** \*Thymoquinone quantity in mg/mL.

**Abbreviations:** HPLC, high-performance liquid chromatography; TQ, thymoquinone.

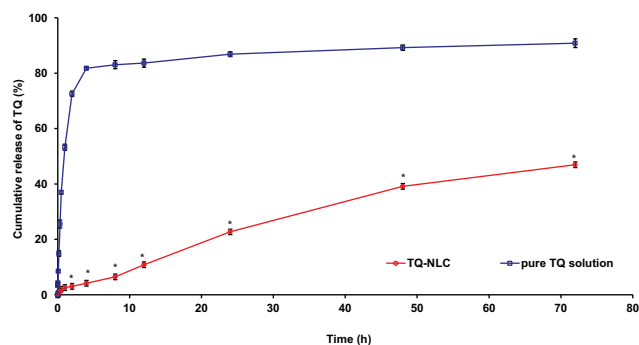


**Figure 1** In vitro drug release profile of TQ-NLC and pure TQ solution. The release of TQ from TQ-NLC was lower than pure TQ solution.

**Notes:** \*  $P < 0.05$ , compared to pure TQ solution.

**Abbreviations:** TQ, thymoquinone; TQNL, TQ-loaded nanostructured lipid carrier.

### Optimization and Stability of Radiolabelling Efficiency

The pharmacokinetics and biodistribution studies were carried out using  $Tc^{99m}$  radiolabeled formulation. In order to ensure the radiolabeled process, the amount of stannous chloride ( $SnCl_2$ ) was critical in this study. During the optimization process, higher amount of  $SnCl_2$  showed high formation of radiocolloids that result in poor radiolabelling efficiency. The optimum labelling efficiency was detected when 150  $\mu g/mL$  of  $SnCl_2$  was used (Table 4). Stability of radiolabeled efficiency reduced over the time up to 24 h but 50% of the content still remained labelled with radioisotope until eight hours when introduced with or without fresh rat serum at 37°C and room temperature (Table 5).

### Pharmacokinetic Study

Following oral and intravenous administration of the radiolabeled TQ-NLC, blood samples were collected at various time intervals and were analysed for %ID/g. The pharmacokinetic profile of  $^{99m}Tc$ -TQ-NLC in blood after the oral and intravenous administration is shown in Figure 3. The data were subjected to calculations of

**Table 3** Linear Regression of TQ-NLC Release Kinetic by Mathematical Modelling Using Various Drug Kinetic Models

| Kinetic Model  | Correlation Coefficient ( $R^2$ ) Value |
|----------------|-----------------------------------------|
| Zero-order     | 0.9710                                  |
| First-order    | 0.5708                                  |
| Higuchi        | 0.9328                                  |
| Hixson–Crowell | 0.7627                                  |

**Abbreviation:** TQ-NLC, thymoquinone-loaded nanostructured lipid carrier.

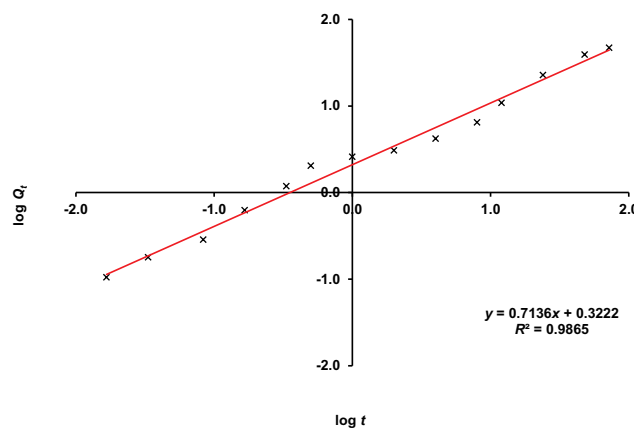


**Figure 2** Linear regression of TQ-NLC release kinetic by using Korsmeyer–Peppas equation. The value of  $n$  was determined from the gradient of the linear line.

**Abbreviation:** TQ-NLC, thymoquinone-loaded nanostructured lipid carrier.

pharmacokinetic parameters based on the noncompartment analysis model.  $C_{max}$ ,  $AUC_{0-\infty}$  and  $t_{1/2}$  (hour) obtained from the percentage of activity levels in blood after oral and intravenous administration of the  $^{99m}Tc$ -TQ-NLC are presented in Table 6. Higher  $C_{max}$  and  $AUC_{0-\infty}$  were obtained following oral administration compared to intravenous administration. The area under the curve ( $AUC_{0-\infty}$ )

**Table 4** Optimisation of Stannous Chloride Amount

| Amount of Stannous Chloride ( $\mu g/mL$ ) | % Drug Labeled (mean $\pm$ SD) |
|--------------------------------------------|--------------------------------|
| 50                                         | 95.69 $\pm$ 0.559              |
| 150                                        | 97.20 $\pm$ 0.115              |
| 300                                        | 92.00 $\pm$ 1.804              |
| 450                                        | 89.53 $\pm$ 2.198              |
| 600                                        | 69.67 $\pm$ 1.859              |

**Note:** Values are expressed as mean  $\pm$ SD and measured in triplicates.

**Table 5** Stability of  $^{99m}Tc$ -TQ-NLC at Room Temperature and in Rat Serum

| Time (hours) | %Labelling Efficiency (mean $\pm$ SD) |                   |
|--------------|---------------------------------------|-------------------|
|              | Room Temperature                      | Rat Serum         |
| 0.5          | 97.22 $\pm$ 0.210                     | 97.22 $\pm$ 0.210 |
| 1            | 93.30 $\pm$ 1.084                     | 80.41 $\pm$ 1.560 |
| 2            | 91.38 $\pm$ 0.445                     | 76.19 $\pm$ 1.413 |
| 4            | 91.27 $\pm$ 0.053                     | 69.05 $\pm$ 2.273 |
| 6            | 84.01 $\pm$ 1.219                     | 66.87 $\pm$ 1.307 |
| 8            | 74.35 $\pm$ 2.324                     | 58.35 $\pm$ 2.616 |
| 24           | 33.43 $\pm$ 1.579                     | 14.92 $\pm$ 2.773 |

**Note:** Values are expressed as mean  $\pm$ SD and measured in triplicates.

**Abbreviations:**  $^{99m}Tc$ , technetium-99m; TQ-NLC, thymoquinone-loaded nanostructured lipid carrier.

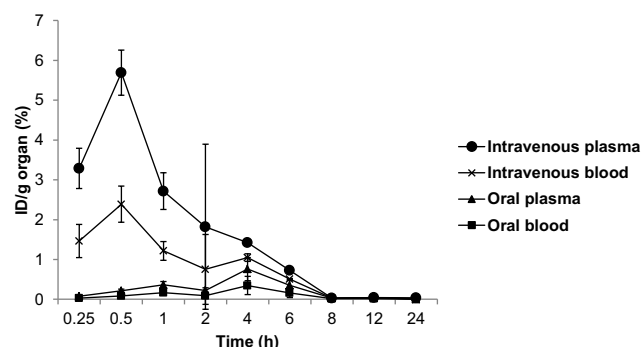


**Figure 3** Time profile of  $^{99m}\text{Tc}$ -TQ-NLC in blood after the oral and intravenous administration into rats ( $n=6$ ).

**Abbreviations:**  $^{99m}\text{Tc}$ , technetium-99m; TQ-NLC, thymoquinone-loaded nanostructured lipid carrier; ID/g, injected dose per gram.

in plasma for intravenous administration of  $^{99m}\text{Tc}$ -TQ-NLC (7.998%ID/g. h) was 4.539 higher compared to the oral administration of radiolabeled TQ-NLC (1.762%ID/g. h). Alternatively, the area under the curve ( $\text{AUC}_{0-\infty}$ ) in blood for intravenous administration of  $^{99m}\text{Tc}$ -TQ-NLC (5.089%ID/g. h) was 3.502 higher compared to the oral administration of radiolabeled TQ-NLC (1.453%ID/g. h). The half-life of  $^{99m}\text{Tc}$ -TQ-NLC both in the plasma and blood after the intravenous administration showed 2.032 and 2.236 times longer half-life respectively, in comparison to the oral administration.

## Biodistribution Study

The biodistribution of  $^{99m}\text{Tc}$ -TQ-NLC over time after the oral administration is shown in Figure 3. The main uptake occurred in the intestine tract. During the first hour following

oral administration, the stomach had high intake of  $^{99m}\text{Tc}$ -TQ-NLC. The concentration of  $^{99m}\text{Tc}$ -TQ-NLC in the intestine increased for the first two hours. Figure 4 shows the distribution of  $^{99m}\text{Tc}$ -TQ-NLC after the intravenous injection. The liver showed an increased uptake over time.  $^{99m}\text{Tc}$ -TQ-NLC consistently accumulated in the kidneys which are clearly visible in all the images except at 24 h. All the aforementioned organs-to-blood and organs-to-muscles for the oral and intravenous administrations showed no significant difference ( $P<0.05$ ) at any time points (Figures 4 and 5).

Besides, the biodistribution of  $^{99m}\text{Tc}$ -TQ-NLC in the intestine, heart, kidneys, liver, lungs, spleen, and stomach after the oral and intravenous administration was also determined using gamma counter analysis to support the images. Depending on the route, the distribution patterns varied (Figures 6 and 7, respectively). Initially, radioactivity of 27.73% and 6.1%, respectively, for the oral and intravenous administration of  $^{99m}\text{Tc}$ -TQ-NLC were observed in the stomach and decreased as the formulations passed through the stomach. In the intestine, there was an increase during the first half hour after the oral administration. However, the radioactivity in the stomach decreased at half to one hour and increased after two hours. After two hours, the radioactivity gradually decreased over time. Different scenario was seen in the intestine after the intravenous administration of  $^{99m}\text{Tc}$ -TQ-NLC where the radioactivity increased for one hour and gradually decreased over time. Another important organ in biodistribution study is liver. Radioactivity in the liver after the oral administration of  $^{99m}\text{Tc}$ -TQ-NLC showed an increase until half an hour and began to decrease thereafter. Moreover, radioactivity in the liver after the intravenous administration of  $^{99m}\text{Tc}$ -TQ-NLC was highest at a quarter of an hour and slowly reduced over time.

**Table 6** Pharmacokinetics Parameters for  $^{99m}\text{Tc}$ -TQ-NLC After Oral and Intravenous Administrations into Rats ( $n=6$ )

| Parameters                          | Oral Administration |         | Intravenous Administration |         |
|-------------------------------------|---------------------|---------|----------------------------|---------|
|                                     | Plasma              | Blood   | Plasma                     | Blood   |
| $T_{\max}$ (h)                      | 4                   | 4       | 0.5                        | 0.5     |
| $C_{\max}$ (%ID/g)                  | 0.413               | 0.347   | 3.284                      | 2.173   |
| $\text{AUC}_{24}$ (%ID/g.h)         | 1.708               | 1.404   | 7.847                      | 4.947   |
| $\text{AUC}_{0-\infty}$ (%ID/g.h)   | 1.762               | 1.453   | 7.998                      | 5.089   |
| $\text{AUC}_{\text{exp}}$ (%ID/g.h) | 3.077               | 3.384   | 1.889                      | 2.788   |
| $t_{1/2}$ (h)                       | 2.457               | 2.386   | 4.992                      | 5.336   |
| CL (L/h)                            | 56.735              | 68.87   | 12.503                     | 19.649  |
| Relative bioavailability (%)        | 201.125             | 236.813 | 90.037                     | 151.259 |

**Abbreviations:**  $\text{AUC}_{24}$ , 24 h area under the curve concentration-time;  $\text{AUC}_{0-\infty}$ , area under the curve to infinity;  $\text{AUC}_{\text{exp}}$ , exponential area under the curve;  $C_{\max}$ , the maximum concentration; CL, clearance; ID/g, injected dose per gram; h, hour;  $^{99m}\text{Tc}$ , technetium-99m; TQ-NLC, thymoquinone-loaded nanostructured lipid carrier;  $T_{\max}$ , the time taken to reach the maximum concentration;  $t_{1/2}$ , half-life.

## Discussion

This study determined the pharmacokinetics and biodistribution of  $^{99m}\text{Tc}$ -TQ-NLC in vivo after oral and intravenous administration. TQ-NLC was successfully synthesized by the hot high-pressure homogenization method.<sup>21</sup> Zeta sizer analysis showed that TQ-NLC has an average diameter of less than 50 nm. TQ-NLC is regarded as nanoparticles according to the European Commission where particles with size ranging from 1–100 nm are categorized as nanoparticles.<sup>48</sup> PDI is an output of autocorrelation function that determines the size distribution range of the particles. The values of PDI were within 0 and 1 where 0 indicates that the nanoparticles are

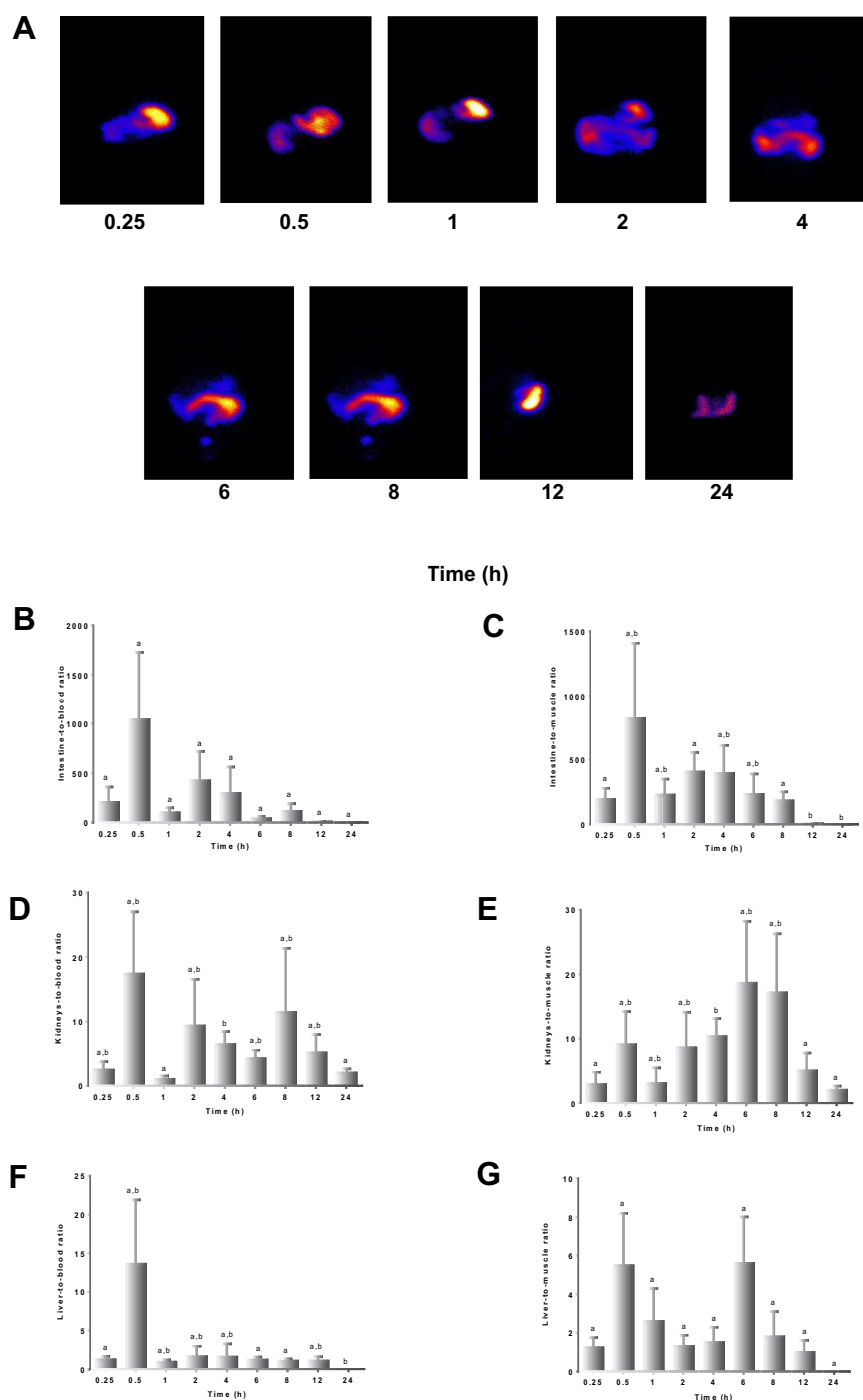


**Figure 4** (A) Images of rats administered with  $^{99m}\text{Tc}$ -TQ-NLC. Gamma camera in vivo data were acquired along 0.25, 0.5, 1, 2, 4, 6, 8, 12, 24 h after the oral administration. (B) Intestine to blood ratios. (C) Intestine to muscle ratios. (D) Liver to blood ratios. (E) Liver to muscle ratios. (F) Kidneys to blood ratios. (G) Kidneys to muscle ratios. **Notes:** Values are expressed as mean  $\pm$ SD,  $n=6$ . Mean values with different letters are significantly different ( $P < 0.05$ ). **Abbreviations:**  $^{99m}\text{Tc}$ , technetium-99m; TQ-NLC, thymoquinone-loaded nanostructured lipid carrier.

highly uniform while 1 indicates the population of nanoparticles is assorted.<sup>49</sup> TQ-NLC has a PDI of less than 0.2.

Another parameter for characterizing nanoparticles is zeta potential, which is measured to determine the surface charge of nanoparticles in a colloidal solution.

A thin layer of counter ions is pulled over by the charge on the surface of the nanoparticles (Stern layer) that move together and disperse throughout the formulation. The zeta potential that contains electric potential within the border of the Stern layer has values that mainly range

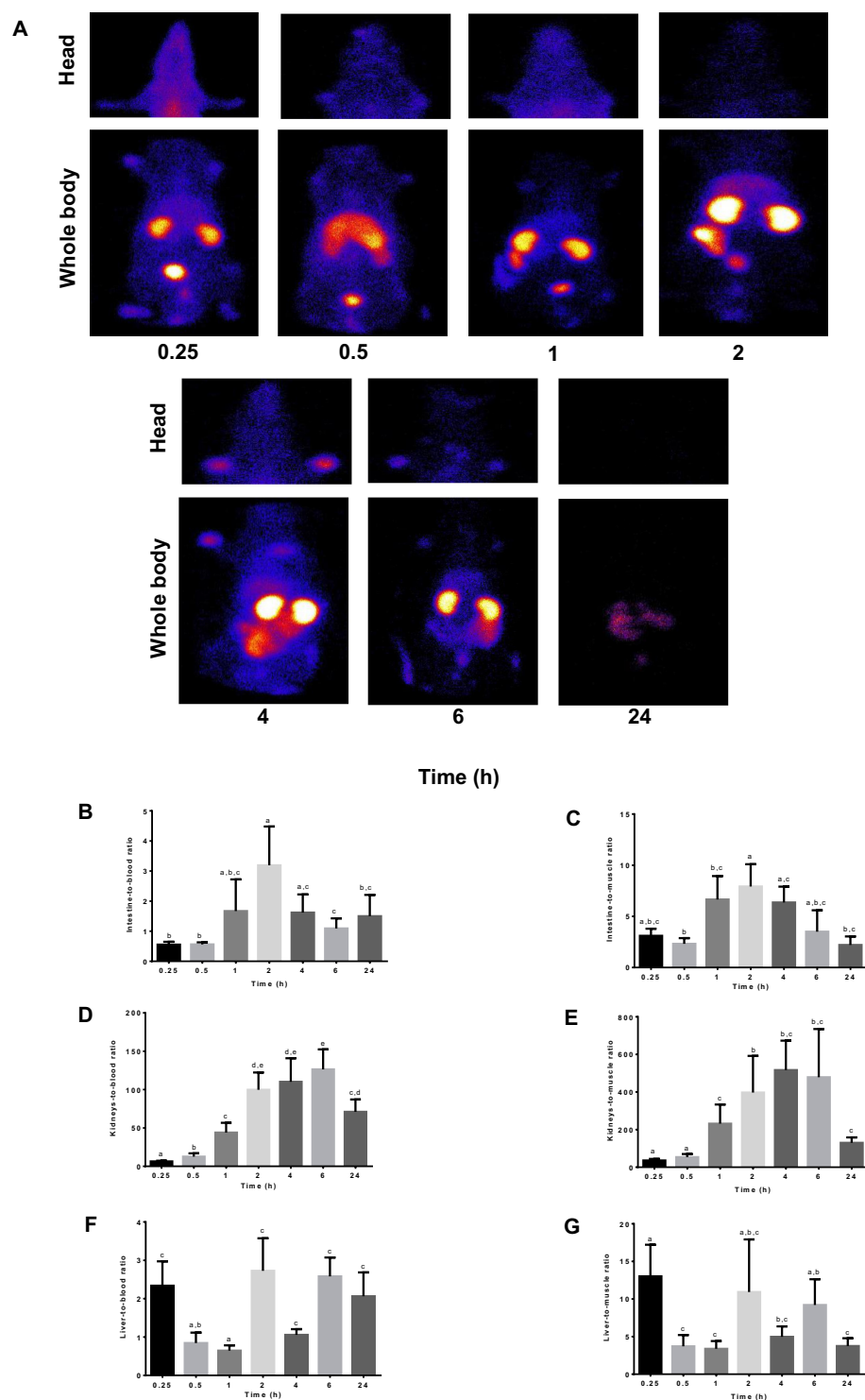


**Figure 5** (A) Images of rats administered with  $^{99m}\text{Tc}$ -TQ-NLC. Gamma camera in vivo data were acquired along 0.25, 0.5, 1, 2, 4, 6, 8, 12, 24 h after the intravenous administration. (B) Intestine to blood ratios. (C) Intestine to muscle ratios. (D) Liver to blood ratios. (E) Liver to muscle ratios. (F) Kidneys to blood ratios. (G) Kidneys to muscle ratios.

**Notes:** Values are expressed as mean  $\pm$ SD,  $n=6$ . Mean values with different letters are significantly different ( $P < 0.05$ ).

**Abbreviations:**  $^{99m}\text{Tc}$ , technetium-99m; TQ-NLC, thymoquinone-loaded nanostructured lipid carrier.

between 100 and  $-100$  mV. The nanoparticles were measured using zeta potential which indicates the colloidal stability.<sup>49</sup> In our study, TQ-NLC has shown a zeta

potential of  $-5.80$  mV. To attain the highest stabilization, zeta potential values of nanoparticles should be greater than positive 30 mV or less than negative 30 mV. Since

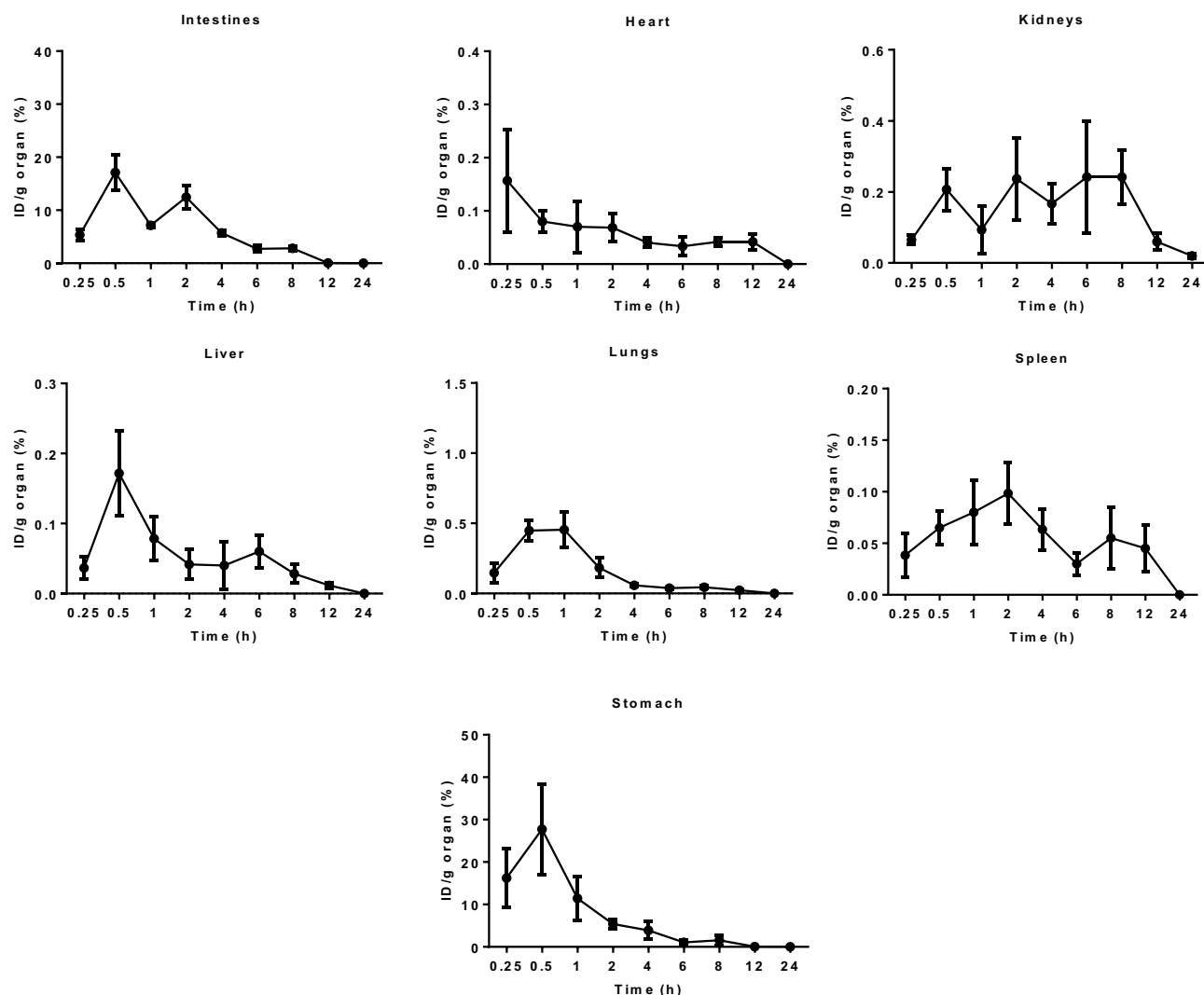


**Figure 6** Biodistribution data showing uptake (% ID/g) of organs vs time profile after the oral administration with  $^{99m}\text{Tc}$ -TQ-NLC (n=6).

**Abbreviations:**  $^{99m}\text{Tc}$ , technetium-99m; TQ-NLC, thymoquinone-loaded nanostructured lipid carrier; ID/g, injected dose per gram.

TQ-NLC has values more than negative 30 mV of zeta potential value, it is considered as an unstable formulation. However, TQ-NLC was stable for up to 24 months (two years) as the average diameter remained lower than 100 nm. Many studies reported that the stability of any nanoparticles does not only depend on the electrostatic repulsion but also involves the use of stabilizer agent. In order to stabilize the dispersion for a longer period, a loss of electrostatic repulsion can be balanced out by using high surfactant mixture.<sup>21,22</sup>

HPLC analysis determines the free TQ which was not encapsulated in the NLC. C18 symmetry analytical column in a mixture of mobile phase of methanol and water (7:3) was used in the analysis.<sup>21,22</sup> High encapsulation of TQ-NLC (98.07%) is possibly because TQ is highly

lipophilic that causes TQ to be attracted to the lipid matrices in the formulation.<sup>50,51</sup> Hence, based on the particles size, PDI, zeta potential and encapsulation efficiency, TQ-NLC can be classified as an ideal nanoformulation with ideal characteristics such as small mean diameter (less than 50 nm), low polydispersity index (less than 0.2), excellent encapsulation and reduced toxicity.<sup>21,22,52</sup> The distribution of the nanoparticles within the body is mainly influenced by these characteristics.<sup>53</sup>

The release profile of TQ-NLC showed that the concentration of TQ released by NLC was not equivalent to the concentration of TQ alone even after 72 h. Hence, in contrast to pure TQ solution (which showed the burst release profile), the absence of concentration spike was anticipated when the cells were treated with TQ-NLC.<sup>54</sup>

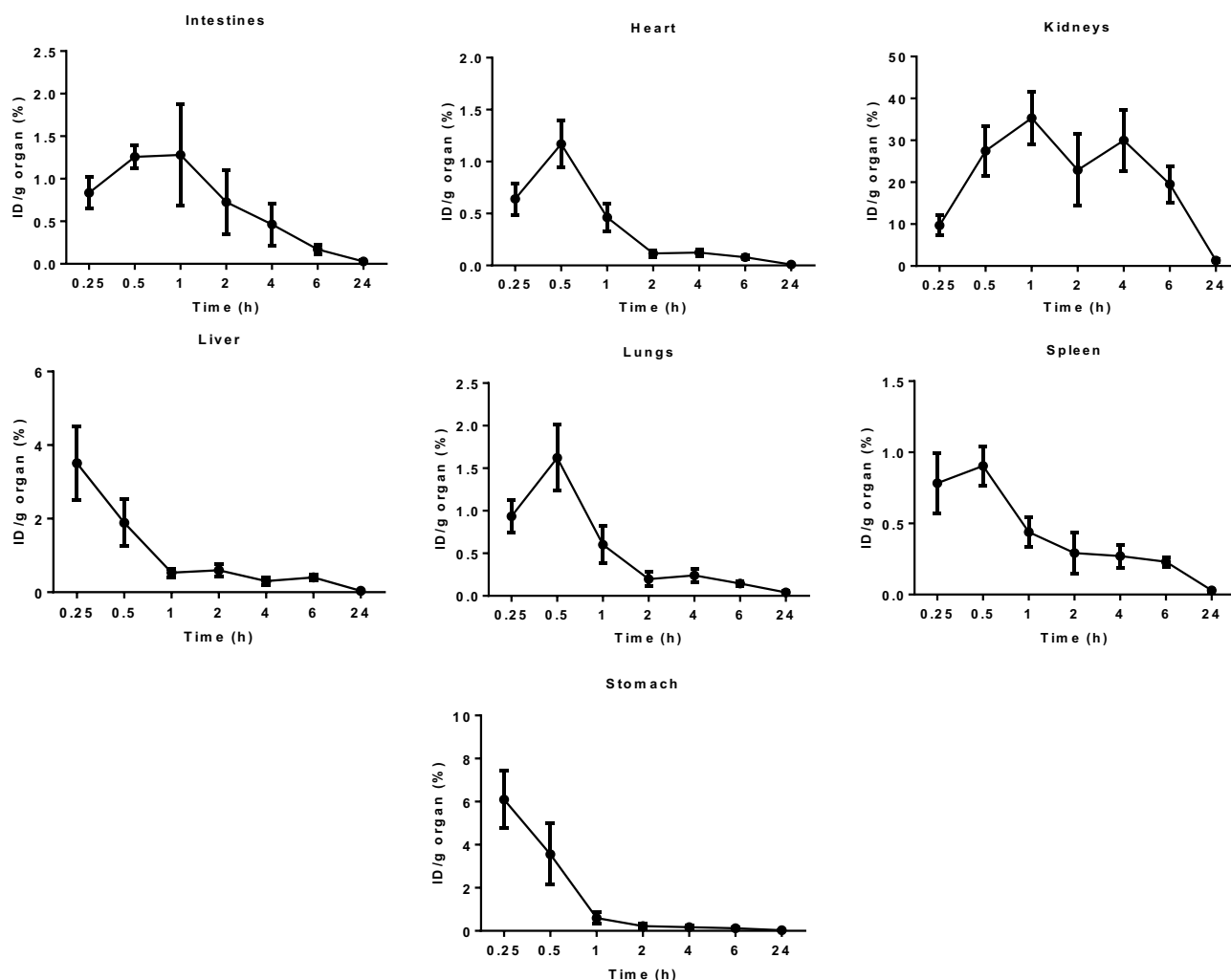


**Figure 7** Biodistribution data showing uptake (% ID/g) of organs vs time profile after the intravenous administration with  $^{99m}\text{Tc}$ -TQ-NLC (n=6). **Abbreviations:**  $^{99m}\text{Tc}$ , technetium-99m; TQ-NLC, thymoquinone-loaded nanostructured lipid carrier; ID/g, injected dose per gram.

In this study, TQ-NLC followed zero-order drug release kinetic since the mathematical modelling and regression analysis revealed that the sustained release of TQ from TQ-NLC was time-dependent and concentration-independent.<sup>21,22</sup> Zero-order drug release kinetic is an ideal sustained delivery system, which prolongs the controlled release of drug from the delivery system and maintains the drug concentration within the therapeutic window, hence, minimizing the episode of toxicity.<sup>55,56</sup>

When administered by the oral route, the main uptake of  $^{99m}\text{Tc}$ -TQ-NLC was in the intestine. This is because  $^{99m}\text{Tc}$ -TQ-NLC is postulated to be taken up by the gastrointestinal tract and move to the reticulum-endothelial organs. This is parallel with previous studies where NLCs were promptly cleared from the systemic circulation by opsonization and taken up by reticulum-endothelial organs.<sup>9,30,57</sup> NLCs are generally accumulated in the

liver and absorbed into the small intestine.<sup>58</sup> Drug-loaded NLCs endure lipid digestion process step by step when they pass through the digestive system. Briefly, triglycerides in the lipid nanoparticles are broken down into monoglycerides and free fatty acids (both long and short chain) caused by the reaction between pancreatic enzymes and molecules within the duodenum that release the drug encapsulated in the NLCs.<sup>59,60</sup> However, it was found that  $^{99m}\text{Tc}$ -TQ-NLC was less accumulated in the liver compared to the intestines within two hours of administration. This is possibly because of the lymphatic intake of  $^{99m}\text{Tc}$ -TQ-NLC within the GI tract passage.  $^{99m}\text{Tc}$ -TQ-NLC can be either absorbed into the portal blood via paracellular route bypassing metabolism due to enterocyte enzymes reactions or can be confined by Peyer's patches (small masses of lymphatic tissue found all over the region in small intestine) that transports  $^{99m}\text{Tc}$ -TQ-NLC to the

lymphatic systems.<sup>44,60</sup> After absorption, long chain fatty acids or lipids are fused into chylomicrons which are then absorbed into the intestinal lymph. Since the size of the chylomicrons are usually large (approximately 80 nm), they enter the lymphatic system instead of blood capillaries that bypass the first metabolism of the drug associated with them.<sup>61</sup>

After administration via intravenous injection, the highest radioactivity levels (expressed as and ID/g tissue) of <sup>99m</sup>Tc-TQ-NLC were observed in the kidney, liver, and spleen. This is supported by previous studies where the nanoparticles were also spotted mainly in these organs of mice after the intravenous administration.<sup>5,60</sup> The presence of the macrophages that reside in these tissues contributes to the uptake into these organs.<sup>62</sup> Since the weight of the kidneys and liver was more prominent compared to others, greater amounts of nanoparticles accumulated in these organs were detected by high levels of radioactivity. Besides, another research also reported high radioactivity levels in the kidneys after nanoparticles administration intravenously<sup>63–65</sup> leads to excretion of the nanoparticles through urine.<sup>5</sup> High radioactivity level detected in the liver is due to the discontinuous liver endothelium that offers a passage for the NLCs as reported by both Beloqui et al and Esposito et al.<sup>5, 9</sup>

Exploring the radioactivity-vs-time profiles, a dip of concentration was found at the first hour in intestines and kidneys (Figure 4B, 4C, 4D and 6). We postulate that <sup>99m</sup>Tc-TQ-NLC gains access into the tissues and organs and formed the first concentration peak. Then the complex returns to the plasma and is redistributed into the tissues and organs causing the second peak. Our finding is in agreement with other researchers that presented similar results suggesting this phenomenon of multiple peaks might be related to the reabsorption of the intestinal tract due to enterohepatic recirculation, variable in gastric emptying and distribution caused by the bile released from the gallbladder. This leads to reabsorption and recycling into the tissue, double-site absorption involving stomach and intestine or variability of absorption. The enterohepatic component associated with the second peak formation includes the gastrointestinal tract and kidneys.<sup>66</sup> A similar pattern of double peak phenomenon in those tissues and organs was also reported by Beloqui et al on biodistribution of nanostructured lipid carriers (NLCs) after intravenous administration to rats.<sup>5</sup>

Furthermore, brain uptake for both routes of administration was less than 0.01% ID/g; a level negligible when

compared with other organs. Therefore, the values were not represented in Figures 6 and 7. Hence, even though there are numerous studies on lipid nanoparticles for brain targeting, factors such as surface charge or the use of polysorbate 80 in the production of this nanoparticle as a stabilizer may hinder the ability of the nanoparticles for brain targeting.<sup>5</sup>

The optimized <sup>99m</sup>Tc-TQ-NLC formulation for pharmacokinetics evaluation showed an area under the curve (AUC<sub>0-∞</sub>) of the intravenous administration which was 4.539 times higher than the oral administration. This indicated that the bioavailability of the intravenous administration of <sup>99m</sup>Tc-TQ-NLC was higher than oral administration. Nanoparticles commonly exist in either positive or negative charges. When administered intravenously, these nanoparticles may bind nonspecifically with various products mainly blood components. Thus, the protein binding influences the distribution of the nanoparticles following the intravenous administration.<sup>5</sup> Higher AUC may be due to lower uptake of the positive nanoparticles by the RES organs (such as liver and spleen) and attract more negative NLC.<sup>5</sup> Besides, the surface properties also play a crucial function when the nanoparticles are in contact with biological fluid such as blood. Generally, a layer of protein known as protein corona will cover the surface of the nanoparticles. The main function of protein corona is to determine the interaction between the nanoparticles and the cell membrane and increase the process of phagocytosis in RES organs.<sup>63,67,68</sup> We postulate that due to lower AUC<sub>0-∞</sub>, the oral administration has slower absorption and better bioavailability compared to intravenous administration. It is parallel with Shah et al who explained that nanoparticles have higher distribution caused by the long circulation time of drug in the blood.<sup>45</sup>

## Conclusion

The NLC drug delivery system is a desired drug carrier for transportation of thymoquinone. TQ-NLC has small size and high encapsulation efficiency where more than 90% of the drug was encapsulated inside NLC. Based on the release profile of TQ-NLC done in vitro, TQ-NLC demonstrated slow and sustained release pattern that possibly can maintain the drug concentration in the therapeutic window. TQ-NLC was absorbed better when administered intravenously compared to oral administration. However oral administration showed greater bioavailability compared to the intravenous route. This study for the very first time provides the

pharmacokinetics and biodistribution profile of TQ-NLC in vivo, which is useful to assist research in clinical use.

## Acknowledgment

This research was supported by RUGS3 (Vote no: 9614500) funded by Universiti Putra Malaysia.

## Disclosure

Prof. Dr Rasheed Abdullah reports a pending patent: Thymoquinone-loaded nanostructured lipid carriers (TQ-NLC) and uses thereof, Malaysian Patent No. P12012001818. The authors report no other potential conflicts of interest in this work.

## References

- Krishnaiah YS. Pharmaceutical Technologies for Enhancing Oral Bioavailability of Poorly Soluble Drugs. *J Bioequiv Availab*. 2010;2(02):28–36. doi:10.4172/jbb.1000027
- Lerisko-iversidge EM, Liversidge GG. Drug Nanoparticles: formulating Poorly Water-Soluble Compounds. *Toxicol Pathol*. 2008;36:43–48. doi:10.1177/0192623307310946
- Zhang L, Gu FX, Chan JM, Wang AZ, Langer RS, Farokhzad OC. Nanoparticles in medicine: therapeutic applications and developments. *Clin Pharmacol Ther*. 2008;83(5):761–769. doi:10.1038/sj.clpt.6100400
- Hirn S, Semmler-Behnke M, Schleh C, et al. Particle size-dependent and surface charge-dependent biodistribution of gold nanoparticles after intravenous administration. *Eur J Pharm Biopharm*. 2011;77(3):407–416. doi:10.1016/j.ejpb.2010.12.029
- Beloqui A, Solinís MA, Delgado A, Évora C, Del Pozo-Rodríguez A, Rodríguez-Gascón A. Biodistribution of Nanostructured Lipid Carriers (NLCs) after intravenous administration to rats: influence of technological factors. *Eur J Pharm Biopharm*. 2013;84(2):309–314. doi:10.1016/j.ejpb.2013.01.029
- Petros RA, Desimone JM. Strategies in the design of nanoparticles for therapeutic applications. *Nat Rev Drug Discov*. 2010;9(8):615–627. doi:10.1038/nrd2591
- Sanvicens N, Marco MP. Multifunctional nanoparticles - properties and prospects for their use in human medicine. *Trends Biotechnol*. 2008;26:425–433. doi:10.1016/j.tibtech.2008.04.005
- Joshi MD, Müller RH. Lipid nanoparticles for parenteral delivery of actives. *Eur J Pharm Biopharm*. 2009;71(2):161–172. doi:10.1016/j.ejpb.2008.09.003
- Esposito E, Boschi A, Ravani L, et al. Biodistribution of nanostructured lipid carriers: A tomographic study. *Eur J Pharm Biopharm*. 2015;89:145–156. doi:10.1016/j.ejpb.2014.12.006
- Owens DE, Peppas NA. Opsonization, biodistribution, and pharmacokinetics of polymeric nanoparticles. *Int J Pharm*. 2006;307(1):93–102. doi:10.1016/j.ijpharm.2005.10.010
- Wissing SA, Kayser O, Rh M. Solid lipid nanoparticles for parenteral drug delivery. *Adv Drug Deliv Rev*. 2004;56(9):1257–1272. doi:10.1016/j.addr.2003.12.002
- Jamal JA, Ghafar ZA, Husain K. Medicinal plants used for postnatal care in Malay traditional medicine in the Peninsular Malaysia. *Pharmacogn J*. 2011;3(24):15–24. doi:10.5530/pj.2011.24.4
- Balaha MF, Tanaka H, Yamashita H, Abdel Rahman MN, Inagaki N. Oral Nigella sativa oil ameliorates ovalbumin-induced bronchial asthma in mice. *Int Immunopharmacol*. 2012;14(2):224–231. doi:10.1016/j.intimp.2012.06.023
- Gali-Muhtasib H, Roessner A. Thymoquinone: S-SR. A promising anti-cancer drug from natural sources. *Int J Biochem Cell Biol*. 2006;38(8):1249–1253. doi:10.1016/j.biocel.2005.10.009
- Ali BH, Blunden G. Pharmacological and toxicological properties of Nigella sativa. *Phyther Res*. 2003;17(4):299–305. doi:10.1002/ptr.1309
- Ahmad A, Husain A, Mujeeb M, et al. A review on therapeutic potential of Nigella sativa: A miracle herb. *Asian Pac J Trop Biomed*. 2013;3(5):337–352. doi:10.1016/S2221-1691(13)60075-1
- Keh ET, Ashour MMS, Al-Harbi MM. The respiratory effects of the volatile oil of the black seed (Nigella sativa) in guinea-pigs: elucidation of the mechanism(s) of action. *Gen Pharmacol*. 1993;24(5):1115–1122. doi:10.1016/0306-3623(93)90358-5
- Radad K, Moldzio R, Taha M, Rausch WD. Thymoquinone protects dopaminergic neurons against MPP+ and rotenone. *Phyther Res*. 2009;23(5):696–700. doi:10.1002/ptr.2708
- Pathan SA, Jain GK, Zaidi SMA, et al. Stability-indicating ultra-performance liquid chromatography method for the estimation of thymoquinone and its application in biopharmaceutical studies. *Biomed Chromatogr*. 2011;25(5):613–620. doi:10.1002/bmc.1492
- Khader M, Bresgen N, Eckl PM. In vitro toxicological properties of thymoquinone. *Food Chem Toxicol*. 2009;47(1):129–133. doi:10.1016/j.fct.2008.10.019
- Ng WK, Saiful Yazan L, Yap LH, et al. Thymoquinone-loaded nanostructured lipid carrier exhibited cytotoxicity towards breast cancer cell lines (MDA-MB-231 and MCF-7) and cervical cancer cell lines (HeLa and SiHa). *Biomed Res Int*. 2015;2015:1–10.
- Ong YS, Saiful Yazan L, Ng WK, et al. Acute and subacute toxicity profiles of thymoquinone-loaded nanostructured lipid carrier in BALB/c mice. *Int J Nanomedicine*. 2016;11:5905–5915. doi:10.2147/IJN.S114205
- Shidhaye S, Vaidya R, Sutar S, Patwardhan A, Kadam V. Solid Lipid Nanoparticles and Nanostructured Lipid Carriers – innovative Generations of Solid Lipid Carriers. *Curr Drug Deliv*. 2008;5(4):324–331. doi:10.2174/156720108785915087
- Patidar A, Thakur DS, Kumar P, Verma J. A review on novel lipid based nanocarriers. *Int J Pharm Pharm Sci*. 2010;2(4):30–35.
- Abdelwahab SI, Sheikh BY, Taha MME, et al. Thymoquinone-loaded nanostructured lipid carriers: preparation, gastroprotection, in vitro toxicity, and pharmacokinetic properties after extravascular administration. *Int J Nanomedicine*;2013. 2163–2172. doi:10.2147/IJN.S44108
- Yoon G, Park JW, Yoon IS. Solid lipid nanoparticles (SLNs) and nanostructured lipid carriers (NLCs): recent advances in drug delivery. *J Pharm Investig*. 2013;43(5):353–362. doi:10.1007/s40005-013-0087-y
- Joshi M, Patravale V. Nanostructured lipid carrier (NLC) based gel of celecoxib. *Int J Pharm*. 2008;346(1–2):124–132. doi:10.1016/j.ijpharm.2007.05.060
- Puri A, Loomis K, Smith B, et al. Lipid-based nanoparticles as pharmaceutical drug carriers: from concepts to clinic. *Crit Rev Ther Drug Carrier Syst*. 2009;26(6):523–580. doi:10.1615/CritRevTherDrugCarrierSyst.v26.i6.10
- Battaglia L, Gallarate M. Lipid nanoparticles: state of the art, new preparation methods and challenges in drug delivery. *Expert Opin Drug Deliv*. 2012;9(5):497–508. doi:10.1517/17425247.2012.673278
- Almeida JPM, Chen AL, Foster A, Drezek R. In vivo biodistribution of nanoparticles. *Nanomedicine*. 2011;6:815–835. doi:10.2217/nnm.11.79
- Hirsjärvi S, Sancey L, Dufort S, et al. Effect of particle size on the biodistribution of lipid nanocapsules: comparison between nuclear and fluorescence imaging and counting. *Int J Pharm*. 2013;453(2):594–600. doi:10.1016/j.ijpharm.2013.05.057

32. Ballot S, Noiret N, Hindré F, et al. 99mTc/188Re-labelled lipid nanocapsules as promising radiotracers for imaging and therapy: formulation and biodistribution. *Eur J Nucl Med Mol Imaging*. 2006;33(5):602–607. doi:10.1007/s00259-005-0007-0
33. Di Domenico G, Zavattini G International Atomic Energy Agency, Vienna (Ed.) *Advances in SPECT Instrumentation (Including Small Animal Scanners)*. Technetium-99m Radiopharmaceuticals: Status and Trends: IAEA Radioisotopes and Radiopharmaceuticals Series No., Austria; 2009:57–90.
34. Saha GB. *Fundamentals of Nuclear Pharmacy*. Springer, New York: The Atom; 2010:1–10.
35. De Barros ALB, De Andrade SF, De Souza Filho JD, Cardoso VN, Alves RJ. Radiolabeling of low molecular weight d-galactose-based glycodendrimer with technetium-99m and biodistribution studies. *J Radioanal Nucl Chem*. 2013;298:605–609. doi:10.1007/s10967-013-2502-2
36. Monteiro LOF, Fernandes RS, Castro LC, et al. Technetium-99 m radiolabeled paclitaxel as an imaging probe for breast cancer in vivo. *Biomed Pharmacother*. 2017;89:146–151. doi:10.1016/j.biopha.2017.02.003
37. Yang DJ, Kim CG, Schechter NR, et al. Imaging with 99m Tc ECDG Targeted at the Multifunctional Glucose Transport System: feasibility Study with Rodents. *Radiology*. 2003;226(2):465–473. doi:10.1148/radiol.2262011811
38. Fani M, Maecke HR. Radiopharmaceutical development of radiolabelled peptides. *Eur J Nucl Med Mol Imaging*. 2012;39(S1):11–30. doi:10.1007/s00259-011-2001-z
39. de Barros ALB, Cardoso VN, Mota L, et al. Synthesis and biodistribution studies of carbohydrate derivatives radiolabeled with technetium-99m. *Bioorganic Med Chem Lett*. 2010;20(1):315–317. doi:10.1016/j.bmcl.2009.10.104
40. Kong FL, Zhang YH, Young DP, Yu DF, Yang DJ. Development of 99mTc-EC-tyrosine for Early Detection of Breast Cancer Tumor Response to the Anticancer Drug Melphalan. *Acad Radiol*. 2013;20(1):41–51. doi:10.1016/j.acra.2012.08.005
41. Dash S, Murthy PN, Nath L, Chowdhury P. Kinetic modeling on drug release from controlled drug delivery systems. *Acta Pol Pharm - Drug Res*. 2010;67(3):217–223.
42. Tigli Aydin RS, Pulat M. 5-fluorouracil encapsulated chitosan nanoparticles for pH-stimulated drug delivery: evaluation of controlled release kinetics. *J Nanomater*. 2012;2012:1–10. doi:10.1155/2012/313961
43. Theobald AE. Quality Control of Radiopharmaceuticals. Textbook of Radiopharmacy: theory and Practice. In: Sampson CB, editor. New York: Gordon and Breach; 1990:115–148.
44. Shah M, Pathak K. Solid Lipid Nanoparticles of Simvastatin: pharmacokinetic and Biodistribution Studies on Swiss albino mice. *Res J Pharm Dos Forms Technol*. 2012;6:336–342.
45. Mishra P, Babbar A, Chauhan U. A rapid instant thin layer chromatographic procedure for determining radiochemical purity of 99mTc-IDA agents. *Nucl Med Commun*. 1991;12(5):467–469. doi:10.1097/00006231-199105000-00013
46. Al-Ali A, Alkhwajah AA, Randhawa MA, Shaikh NA. Oral and intraperitoneal LD50 of thymoquinone, an active principle of *Nigella sativa*, in mice and rats. *J Ayub Med Coll Abbottabad*. 2008;20(2):25–27.
47. Yazan LS, Mohd Azlan SN, Zakarial Ansar FH, Gopalsamy B. Acute toxicity study of intravenous administration of thymoquinone-loaded nanostructured lipid carrier (TQ-NLC) in Sprague Dawley rats. *Malaysian J Med Heal Sci*. 2019;15(2):51–57.
48. Commission Recommendation of 18 October 2011 on the definition of nanomaterial Text with EEA relevance Official Journal of the European Union 275. 2011:38–40.
49. Kumar A, Dixit CK. Methods for characterization of nanoparticles. In: *Advances in Nanomedicine for the Delivery of Therapeutic Nucleic Acids*. 2017:44–58.
50. Paini M, Daly SR, Aliakbarian B, et al. An efficient liposome based method for antioxidants encapsulation. *Colloids Surf B Biointerfaces*. 2015;136:1067–1072. doi:10.1016/j.colsurfb.2015.10.038
51. Müller RH, Radtke M, Sa W. Solid lipid nanoparticles (SLN) and nanostructured lipid carriers (NLC) in cosmetic and dermatological preparations. *Adv Drug Deliv Rev*. 2002;54(1):131–155. doi:10.1016/S0169-409X(02)00118-7
52. Ong YS, Yazan LS, Ng WK, et al. Thymoquinone loaded in nanostructured lipid carrier showed enhanced anticancer activity in 4T1 tumor-bearing mice. *Nanomedicine*. 2018;13(13):1567–1582. doi:10.2217/nmm-2017-0322
53. Montaner J, Cano-Sarabia M, Simats A, et al. Charge effect of a liposomal delivery system encapsulating simvastatin to treat experimental ischemic stroke in rats. *Int J Nanomedicine*. 2016;11:3035–3048. doi:10.2147/IJN.S107292
54. How CW, Rasedee A, Manickam S, Rosli R. Rosli R: tamoxifen-loaded nanostructured lipid carrier as a drug delivery system: characterization, stability assessment and cytotoxicity. *Coll Surf B*. 2013;112:393–399. doi:10.1016/j.colsurfb.2013.08.009
55. Araújo J, Garcia ML, Mallandrich M, Souto EB, Calpena AC. Calpena AC: release profile and transscleral permeation of triamcinolone acetonide loaded nanostructured lipid carriers (TA-NLC): in vitro and ex vivo studies. *Nanomed Nanotechnol Biol Med*. 2012;8(6):1034–1041. doi:10.1016/j.nano.2011.10.015
56. Siegel RA. Rathbone MJ: overview of Controlled Release Mechanisms. In: *Fundamentals and Applications of Controlled Release*. 2012:19–44.
57. Iqbal MA, Md S, Sahni JK, Baboota S, Dang S, Ali J. Nanostructured lipid carriers system: recent advances in drug delivery. *J Drug Target*. 2012;20(10):813–830. doi:10.3109/1061186X.2012.716845
58. Yang S, Zhu J, Lu Y, Liang B, Yang C. Body distribution of camptothecin solid lipid nanoparticles after oral administration. *Pharm Res*. 1999;16(5):751–757. doi:10.1023/A:1018888927852
59. Neelam S, Hayes PR, Zhang Q, Dickinson RB, Lele TP. Vertical uniformity of cells and nuclei in epithelial monolayers. *Sci Rep*. 2016;6(1):19689. doi:10.1038/srep19689
60. Yao M, McClements DJ, Xiao H. Improving oral bioavailability of nutraceuticals by engineered nanoparticle-based delivery systems. *Curr Opin Food Sci*. 2015;2:14–19. doi:10.1016/j.cofs.2014.12.005
61. Chen LC, Wu YH, Liu IH, et al. Pharmacokinetics, dosimetry and comparative efficacy of 188Re-liposome and 5-FU in a CT26-luc lung-metastatic mice model. *Nucl Med Biol*. 2012;39:35–43. doi:10.1016/j.nucmedbio.2011.06.010
62. Li SD, Huang L. Pharmacokinetics and biodistribution of nanoparticles. *Mol Pharm*. 2008;5(4):496–504. doi:10.1021/mp800049w
63. Cole AJ, David AE, Wang J, Galbán CJ, Yang VC. Magnetic brain tumor targeting and biodistribution of long-circulating PEG-modified, cross-linked starch-coated iron oxide nanoparticles. *Biomaterials*. 2011;32(26):6291–6301. doi:10.1016/j.biomaterials.2011.05.024
64. Snehaltha M, Venugopal K, Saha RN, Babbar AK, Sharma RK. Etoposide loaded PLGA and PCL nanoparticles II: biodistribution and pharmacokinetics after radiolabeling with Tc-99m. *Drug Deliv*. 2008;15(5):277–287. doi:10.1080/10717540802006500
65. Yan C, Gu J, Guo Y, Chen D. In Vivo Biodistribution for Tumor Targeting of 5-Fluorouracil (5-FU) Loaded N-succinyl-chitosan (Suc-Chi) Nanoparticles. *Yakugaku Zasshi*. 2010;130(6):801–804. doi:10.1248/yakushi.130.801

66. Davies NM, Takemoto JK, Brocks DR, Yáñez JA. Multiple peaking phenomena in pharmacokinetics disposition. *Clini Pharmacokinet.* 2010;49(6):351–377. doi:10.2165/11319320-000000000-00000
67. Özcan I, Segura-Sánchez F, Bouchemal K, et al. Pegylation of poly ( $\gamma$ -benzyl-L-glutamate) nanoparticles is efficient for avoiding mononuclear phagocyte system capture in rats. *Int J Nanomedicine.* 2010;5:1103–1111. doi:10.2147/IJN.S15493
68. Kang H, Mintri S, Menon AV, Lee HY, Choi HS, Kim J. Pharmacokinetics, pharmacodynamics and toxicology of theranostic nanoparticles. *Nanoscale.* 2015;7(45):18848–18862. doi:10.1039/C5NR05264E

### International Journal of Nanomedicine

Dovepress

### Publish your work in this journal

The International Journal of Nanomedicine is an international, peer-reviewed journal focusing on the application of nanotechnology in diagnostics, therapeutics, and drug delivery systems throughout the biomedical field. This journal is indexed on PubMed Central, MedLine, CAS, SciSearch®, Current Contents®/Clinical Medicine,

Journal Citation Reports/Science Edition, EMBase, Scopus and the Elsevier Bibliographic databases. The manuscript management system is completely online and includes a very quick and fair peer-review system, which is all easy to use. Visit <http://www.dovepress.com/testimonials.php> to read real quotes from published authors.

Submit your manuscript here: <https://www.dovepress.com/international-journal-of-nanomedicine-journal>